The American Journal of Sports Medicine

http://ajs.sagepub.com/

One-Year Outcomes of Total Meniscus Reconstruction Using a Novel Fiber-Reinforced Scaffold in an Ovine Model

Jay M. Patel, Aaron R. Merriam, Brian M. Culp, Charles J. Gatt, Jr and Michael G. Dunn

Am J Sports Med 2016 44: 898 originally published online February 3, 2016
DOI: 10.1177/0363546515624913

The online version of this article can be found at:
http://ajs.sagepub.com/content/44/4/898

Published by:

http://www.sagepublications.com

On behalf of:

American Orthopaedic Society for Sports Medicine

Additional services and information for *The American Journal of Sports Medicine* can be found at:

Email Alerts: http://ajs.sagepub.com/cgi/alerts

Subscriptions: http://ajs.sagepub.com/subscriptions

Reprints: http://www.sagepub.com/journalsReprints.nav

Permissions: http://www.sagepub.com/journalsPermissions.nav

>> Version of Record - Mar 31, 2016

OnlineFirst Version of Record - Feb 26, 2016

OnlineFirst Version of Record - Feb 3, 2016

What is This?

Downloaded from ajs.sagepub.com at RUTGERS UNIV on April 5, 2016

One-Year Outcomes of Total Meniscus Reconstruction Using a Novel Fiber-Reinforced Scaffold in an Ovine Model

Jay M. Patel,*† ME, Aaron R. Merriam,*† PhD, Brian M. Culp,* MD, Charles J. Gatt Jr,*† MD, and Michael G. Dunn,*†‡ PhD
Investigation performed at Rutgers Biomedical and Health Sciences–Robert Wood Johnson Medical School, New Brunswick, New Jersey, USA

Background: Meniscus injuries and resulting meniscectomies lead to joint deterioration, causing pain, discomfort, and instability. Tissue-engineered devices to replace the meniscus have not shown consistent success with regard to function, mechanical integrity, or protection of cartilage.

Purpose: To evaluate a novel resorbable polymer fiber–reinforced meniscus reconstruction scaffold in an ovine model for 52 weeks and assess its integrity, tensile and compressive mechanics, cell phenotypes, matrix organization and content, and protection of the articular cartilage surfaces.

Study Design: Controlled laboratory study.

Methods: Eight skeletally mature ewes were implanted with the fiber-reinforced scaffold after total meniscectomy, and 2 additional animals had untreated total meniscectomies. Animals were sacrificed at 52 weeks, and the explants and articular surfaces were analyzed macroscopically. Explants were characterized by ultimate tensile testing, confined compression creep testing, and biochemical, histological, and immunohistochemical analyses. Cartilage damage was characterized using the Mankin score on histologic slides from both the femur and tibia.

Results: One sheep was removed from the study because of a torn extensor tendon; the remaining 7 explants remained fully intact and incorporated into the bone tunnels. All explants exhibited functional tensile loads, tensile stiffnesses, and compressive moduli. Fibrocartilagenous repair with both types 1 and 2 collagen were observed, with areas of matrix organization and biochemical content similar to native tissue. Narrowing in the body region was observed in 5 of 7 explants. Mankin scores showed less cartilage damage in the explant group (femoral condyle: 3.43 $\pm$ 0.79, tibial plateau: 3.50 $\pm$ 1.63) than in the meniscectomy group (femoral condyle: 8.50 $\pm$ 3.54, tibial plateau: 6.75 $\pm$ 2.47) and were comparable with Mankin scores at the previously reported 16- and 32-week time points.

Conclusion: A resorbable fiber-reinforced meniscus scaffold supports formation of functional neomeniscus tissue, with the potential to prevent joint degeneration that typically occurs after total meniscectomy. Further studies with improvements to the initial mechanics of the scaffold and testing for longer time periods are warranted.

Clinical Relevance: Meniscectomy is an extremely common orthopaedic procedure, and few options currently exist for the treatment of significant loss of meniscus tissue. Successful development of a tissue-engineered meniscus scaffold could substantially reduce the incidence of postmeniscectomy joint degeneration and the subsequent procedures used for its treatment.

Keywords: meniscus; tissue engineering; biomechanics; knee

Meniscus tears are one of the most common musculoskeletal injuries. Because of the relative avascularity of the meniscus,[2] tears are often unable to heal without surgical intervention, causing patients pain and loss of mobility. Meniscectomy is one of the most frequently performed orthopaedic procedures and involves removing the damaged tissue.[12] Although meniscectomy has shown short-term symptom relief, long-term follow-up shows a direct correlation between the amount of meniscus tissue removed and the amount of articular cartilage damage.[1,17] Another option for large meniscus tears is allograft transplantation, which provides a fully intact, mechanically functional total meniscus replacement.[37] However, disadvantages include long-term failure, limited cellular infiltration and remodeling, size-matching issues, graft preservation, and risk of disease transmission. Recent advances in tissue engineering may provide an off-the-shelf, cell-free meniscus replacement that provides long-term cartilage protection and prevents the onset of osteoarthritis.

The American Journal of Sports Medicine, Vol. 44, No. 4
DOI: 10.1177/0363546515624913
© 2016 The Author(s)

Downloaded from ajs.sagepub.com at RUTGERS UNIV on April 5, 2016

The menisci of the knee aid in load distribution, stability, lubrication, and joint preservation.[28] The menisci protect the articular surfaces by distributing loads from the femoral condyle over a larger area on the tibial plateau. One critical property of the meniscus is its ability to resist tension when compressive stresses are converted to circumferential hoop stresses.[32,40] Therefore, tissue-engineering approaches should aim to replicate these mechanical functions. Two of the first clinically used implants were the collagen-based Menaflex[38,39] and the polyurethane-based Actifit.[8,9] Both implants are porous sponges that are conducive to cellular ingrowth.[43] However, because of the relatively low circumferential tensile mechanics of these isotropic sponges, their use is limited to partial meniscus replacement, requiring an intact peripheral meniscus rim.

Previous tissue-engineering strategies have used biological materials such as collagen,[3,14] hyaluronan,[7,11] and silk[29] and synthetic polymers such as polylactic acid,[7] polyglycolic acid,[11,23] polycaprolactone,[7,22,26] polyethylene,[19] and poly vinyl alcohol.[19] While several short-term (<8-month) studies have shown compressive resistance, fibrochondrocytic cell morphology, and collagen expression, most have failed at longer time points because of implant rupture and/or joint deterioration.[44] These shortcomings are often attributed to an inability to provide and maintain functional tensile mechanics.

Previously, our group developed a total meniscus replacement device composed of a collagen-hyaluronan sponge reinforced with degradable poly (desaminotyrosyl-tyrosine dodecyl ester dodecanoate) (pDTDDD) fibers oriented to mimic the structure of the meniscus.[4] The novel implant design is patented (US Patent No. US8623085 B2[13]) and has been licensed for product development (Meniscofix; Novopedics Inc). The porous sponge provides a substrate for cell attachment and infiltration. pDTDDD is a tyrosine-derived polymer that has relatively high mechanical properties and a relatively slow degradation profile.[5] The reinforced scaffold was shown to exhibit an ultimate tensile load and tensile stiffness similar to the native meniscus. An ovine total meniscus replacement study demonstrated the success of this scaffold, particularly with regard to affinity for cellular infiltration and matrix deposition, maintenance of functional mechanical loads, and protection of the articular cartilage compared with untreated meniscectomies at 16 and 32 weeks postoperatively.[31]

The purpose of this study was to evaluate this implant for 52 weeks in an ovine model and make comparisons to the previous 16- and 32-week results as well as to 52-week untreated meniscectomy. Our hypothesis was that the meniscus scaffold would be able to (1) remain intact and incorporate into the bone tunnels, (2) maintain functional tensile properties, (3) have compressive properties that approximate those of native tissue, (4) become populated with fibrochondrocytic cells and exhibit extracellular matrix (ECM) deposition and organization, and (5) improve cartilage protection compared with meniscectomy while preventing the progression of cartilage damage.

METHODS

In this study, we implanted scaffolds into 8 sheep. In addition, we performed untreated total meniscectomies on 2 additional sheep to verify cartilage damage after meniscectomy in this animal model. An ovine model was used because of the similarities in meniscus structure between sheep and humans.[6] Upon retrieval at 52 weeks postoperatively, uniaxial tensile testing and confined compression creep testing were performed. Histological staining was performed to analyze the cellular and extracellular makeup of the explanted neomeniscus tissue. Immunohistochemistry was performed to examine distribution of collagen types 1 and 2 (COL-1, COL-2). Collagen and sulfated glycosaminoglycans (S-GAG) content were obtained through colorimetric assays. The femoral and tibial articular cartilage of the experimental and meniscectomy groups was analyzed histologically for damage using Mankin scores.

Scaffold Production

The pDTDDD was polymerized, melt extruded, and drawn into 100-μm-diameter fiber at the New Jersey Center for Biomaterials (Department of Chemistry, Rutgers University). Fiber was quasi-woven around a circumferential set of pins to create a semilunar, wedge-shaped network of fibers,[4] with extended tails for fixation (Figure 1). A slight modification was made to the scaffold used in the previous ovine study.[31] Additional fiber was added primarily to the inner margin of the scaffold (Figure 1), resulting in a 28% increase in total fiber length.

Sodium hyaluronate (molecular weight 1.5-2.2 MDa; 0.25 g/L; Acros Organic) from bacterial fermentation was dissolved in dilute hydrochloric acid (HCl; pH 2.35). Ground, lyophilized type I bovine Achilles tendon collagen (20 g/L, 2% wt/vol; Worthington Biochemical Corp) was swollen in the hyaluronic acid solution. The gel-like dispersion was injected into and around the quasi-woven scaffold. The scaffold was frozen via ethanol–dry ice bath and lyophilized (–50°C, 0.05 mbar) for 24 hours. Scaffolds were crosslinked in 1-ethyl-3-(dimethyl aminopropyl) carbodiimide

‡Address correspondence to Michael G. Dunn, PhD, Department of Orthopaedic Surgery, Rutgers Biomedical and Health Sciences–Robert Wood Johnson Medical School, 51 French Street, MEB 424, New Brunswick, NJ 08903, USA (email: dunnmg@rwjms.rutgers.edu).

*Department of Orthopaedic Surgery, Rutgers Biomedical and Health Sciences–Robert Wood Johnson Medical School, New Brunswick, New Jersey, USA.

†Department of Biomedical Engineering, Rutgers–The State University of New Jersey, Piscataway, New Jersey, USA.

One or more of the authors has declared the following potential conflict of interest or source of funding: Research was funded by the Armed Forces Institute for Regenerative Medicine (AFIRM I, grant W81XWH-08-2-0034). The funding agency did not play a role in the investigation. C.J.G. is on the board of directors of, is interim president of, and owns stock in NovoPedics Inc, a startup company developing the meniscus implant for potential future commercialization. M.G.D. is interim secretary of and owns stock in NovoPedics Inc. Neither receives any salary from the company. C.J.G. and M.G.D. are inventors on 2 United States patents, and A.R.M. is an inventor on 1 United States patent for the meniscus implant described in the article.

Downloaded from ajs.sagepub.com at RUTGERS UNIV on April 5, 2016

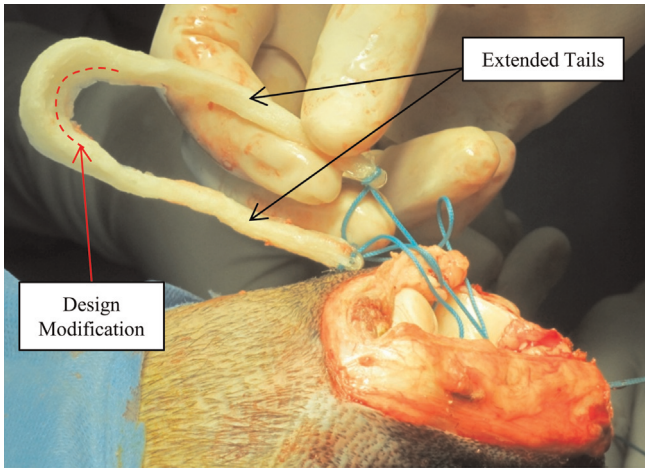

Figure 1. Implantation of the fiber-reinforced scaffold in an ovine model. The extended tails (black arrows) were fixed in tibial bone tunnels with titanium interference screws. The design modification was fiber addition to the inner margin of the scaffold (red dotted line).

(10 mM) and N-hydroxysuccinimide (5 mM) for 6 hours (50 mL per scaffold). Scaffolds were subjected to three 10-minute washes in DI H_2O, a 3-hour sodium phosphate wash (Na_2HPO_4; 100 mM), and four 6-hour DI H_2O washes. Last, scaffolds were lyophilized again and sterilized with gamma irradiation (Sterigenics) at 25 kGy.

Surgical Procedure and Sacrifice

Ten skeletally mature (2-3 years; 50-70 kg) Dorset Finn Cross sheep were used in this study under an Institutional Animal Care and Use Committee–approved protocol, with 8 sheep receiving an implant (experimental group) and 2 sheep receiving an untreated meniscectomy. Surgical preparation, procedure, and postoperative care were performed as previously described.[31] Animals were anesthetized and each right hindlimb was scrubbed and sterilely prepared. Total medial meniscectomies were performed on the right hindlimb of all animals. For the experimental group, tibial bone tunnels were drilled at the anterior and posterior horn sites. The scaffold tails (Figure 1) were pulled through the tunnels and fixed with titanium interference screws (Smith & Nephew). Animals were allowed unrestricted movement 3 hours after the procedure and given antibiotic, anti-inflammatory, and pain-killing medication as necessary. Animals were sent to a farm facility approximately 2 weeks postoperatively and were sacrificed at 52 weeks. Explants were analyzed macroscopically for intactness, size, and shape and evaluated mechanically, biochemically, and histologically. The articular surfaces from all 10 sheep were recovered. The 10 native medial menisci extracted from the surgeries (right leg) were also analyzed: 4 for tensile testing, 4 for compression creep and biochemical testing, and 2 for histology and immunohistochemistry. Surgeries and postoperative care were performed by the same orthopaedic surgeon and staff to minimize variability.

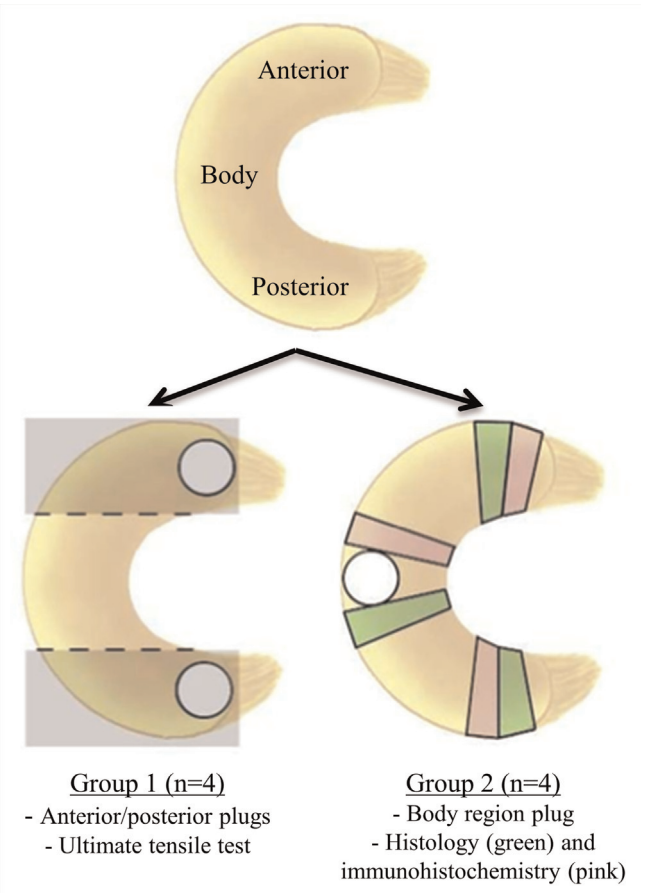

Figure 2. Explant groups. Group 1: Anterior and posterior plugs taken for confined compressive creep/biochemical testing and remainder for ultimate tensile testing. Group 2: Body plug for confined compressive creep/biochemical testing and 2 slices per region (anterior, body, posterior) for histology and immunohistochemistry.

Mechanical Evaluation

The mechanical properties of the explants were characterized using uniaxial tensile testing and confined compressive creep testing. Explants were randomly assigned to 1 of 2 groups (n = 4 per group) (Figure 2). From the first group, cylindrical plugs (4-mm diameter × 4-mm height) were taken from the anterior and posterior regions and used for confined compressive creep testing. Uniaxial tensile testing was performed on those 4 explants, 4 native menisci, and 4 unimplanted scaffolds (after sterilization). The anterior and posterior regions were loaded into cryoclamps (Bose ElectroForce Systems) with a 10-mm–gauge length consisting of the sample's body region (Figure 2, left). All samples were tested (Instron No. 5569) at 10 mm/min until failure. Load at failure and tensile stiffness were obtained.

Downloaded from ajs.sagepub.com at RUTGERS UNIV on April 5, 2016

From the second group of 4 explants, 1 additional plug was taken from the body region to obtain 4 plugs per region. Anterior, body, and posterior plugs were also taken from each of 4 native menisci. For confined compressive creep testing, samples were hydrated for at least 60 minutes and placed in a 4-mm-diameter cylindrical chamber with a unidirectional fluid flow filter. A 1-N load was applied for 3600 seconds (Instron No. 5542). The aggregate moduli of the samples were calculated using the biphasic theory of Mow et al.[33]

Histological Evaluation

The remaining tissue from the second group of explants was used for histological and immunohistochemical evaluation (Figure 2). Two tissue samples were taken from the anterior, body, and posterior regions. One sample from each region was fixed in Carson's buffered formalin, paraffin embedded, cut into 8-μm-thick radial cross sections, and stained with hematoxylin and eosin (AML Laboratories). Polymer fiber density was obtained by taking 5 randomly chosen images (2.36 mm^2) from the anterior, body, and posterior regions of each of the 4 explants. The number of fibers in each image was counted, and density was calculated and averaged over the 5 images. The slides were also analyzed qualitatively for cell concentration and morphology, ECM development and organization, vascularity, and inflammatory response.

The second tissue sample from each region was embedded in optimal cutting temperature compound (Tissue-Tek; Sakura) and frozen with liquid N_2. After fixation in 100% methanol for 10 minutes, 8-μm-thick sections were cut and stained for COL-1 (AB745; Millipore) and COL-2 (AB34712; Abcam Inc) and with secondary fluorescent antibody (AlexaFluor 594; Texas Red; Life Technologies). Autofluorescence was negated by using negative controls to set the exposure. The location and content of each collagen type were observed qualitatively. Differences between the inner and outer margins and between the regions were also noted. Explant sections were also compared with those of native menisci for both methods of staining.

Biochemical Testing: Collagen and GAG Content

For quantitative biochemical analyses, compression creep plugs (explant and native tissue) were frozen and lyophilized. These samples were weighed (10-25 mg each) and digested with papain solution (1 mg tissue/100 μL solution; 125 μg/mL papain, 5 mM L-cysteine-HCl, 5 mM ethylenediaminetetraacetic acid disodium salt (EDTA-2Na) in phosphate-buffered saline, pH 6.0) for 24 hours. The 100-μL sample homogenates were hydrolyzed with 100 μL of 12 M HCl at 120°C for 24 hours. Two 10-μL aliquots from each hydrolyzed sample were transferred to a 96-well plate and evaporated to dryness under vacuum. Each well (including 2 blank wells and 7 × 2 standard wells) was subject to incubation in 100 μL chloramine T (20 minutes, room temperature) followed by incubation in 100 μL dimethylaminobenzaldehyde (30 min, 60°C). Absorbance was measured at 530 nm, and hydroxyproline concentration per gram of tissue was used to calculate collagen content with a scale factor of 7.46.[34] Two additional 100-μL sample homogenates were stained with 100 μL of 1,9 dimethylmethylene blue. Absorbance was measured immediately at 525 nm, and S-GAG concentration per gram of tissue was calculated. Concentrations were calculated by using a regression analysis on ranges of hydroxyproline and chondroitin-6-sulfate standards.

Articular Cartilage Evaluation

After explant recovery, the femoral condyle and tibial plateau of each knee were analyzed macroscopically for location (International Cartilage Repair Society [ICRS] mapping system) of damage. Anterior-to-posterior slices were taken from the femoral condyle and tibial plateau of all 10 sheep (8 experimental, 2 meniscectomy). Slices were fixed in Carson's buffered formalin and embedded in paraffin, and 8 μm sections were stained with Safranin O/Fast Green (AML Laboratories). The central region of each section was graded with the Mankin score,[30] a semiquantitative system ranging from 0 (no damage) to 14 (complete damage) that accounts for structural damage, cellular changes, proteoglycan stain, and tidemark integrity.

Statistical Analyses

Explant ultimate tensile load and tensile stiffness were analyzed with a 1-factor analysis of variance (ANOVA; $P < .05$) when being compared with native and time-zero (unimplanted scaffold) values. A post hoc Tukey honest significant difference (HSD) test was performed to find statistical differences between groups. Regional differences (between anterior, body, and posterior regions) in fiber densities and biochemical data from the explant group were compared with 1-factor ANOVA with Tukey HSD. Aggregate moduli and biochemical content from the anterior, body, and posterior regions were compared between native menisci and explant tissue with a 2-tailed, type 2 t test ($P < .05$).

RESULTS

Macroscopic Observations

All animals returned to a standing position within 3 hours postoperatively and achieved normal weightbearing and gait within 6 weeks. All animals experienced slight weight gain but only by an average of 10.1%. One sheep was removed from the experimental group because of a torn extensor tendon that may have been caused by interference screw placement. This resulted in 3 explants for tensile analysis, 3 anterior and 3 posterior plugs for compressive analysis, and 7 experimental articular surfaces for cartilage analysis. At sacrifice, all 7 explants were fully intact, firmly anchored to the bone tunnels, and peripherally attached to the tibial plateau at the capsular junction. Tissue infiltration was observed and fibers remained present, especially at the bone tunnel

Downloaded from ajs.sagepub.com at RUTGERS UNIV on April 5, 2016

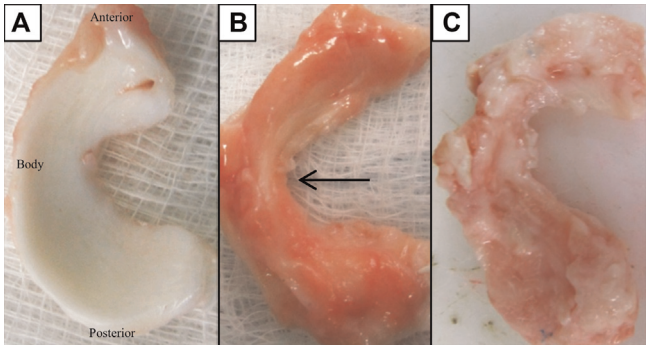

Figure 3. Macroscopic images of (A) native ovine meniscus, (B) a 52-week explant with narrowing (arrow), and (C) 52-week meniscectomy scar tissue growth.

attachment sites. Five of the 7 explants experienced narrowing in the body region, as shown with a black arrow in Figure 3. This narrowing was classified as a decrease in inner margin–to–outer margin width. The meniscectomy sheep experienced scar tissue growth into the space left after meniscectomy. This tissue was rough and spongy in comparison with the native meniscus and explants and upon handling had very little mechanical integrity. Images of a native meniscus, an explant example with narrowing in the body region, and a meniscectomy scar tissue example can be seen in Figure 3.

Mechanical Evaluation

Unimplanted (time-zero) scaffolds possessed a similar ultimate tensile load and significantly higher tensile stiffness compared with native menisci. The ultimate tensile load was significantly lower for explants (210.4 ± 14.0 N) than for both the native menisci (572.6 ± 210.9 N) and time-zero scaffolds (524.6 ± 48.6 N) (Figure 4A). The tensile stiffness of explants (66.1 ± 32.5 N/mm) was significantly lower than native menisci (143.5 ± 41.6 N/mm) and time-zero scaffolds (249.4 ± 34.1 N/mm) (Figure 4A).

The 52-week explant plugs had an average aggregate modulus (0.40 ± 0.19 MPa) that was 51% that of the native meniscus (0.78 ± 0.25 MPa) (Figure 4B). The aggregate moduli of the anterior and body regions of the explants were significantly lower than that of native tissue, and the posterior region had the highest aggregate modulus (0.59 ± 0.24 MPa) of the 3 explant regions.

Histological Evaluation

A characteristic histology image for each explant region (anterior, body, posterior), accompanied by that group's average polymer fiber density, is shown along with an image from a native meniscus in Figure 5. The anterior region had a significantly greater polymer fiber density than the body and posterior regions. Polymer fibers in the anterior region maintained diameters between 100 and 110 μm, whereas some fibers from the body and posterior regions had diameters <50 μm. Polymer fibers tended

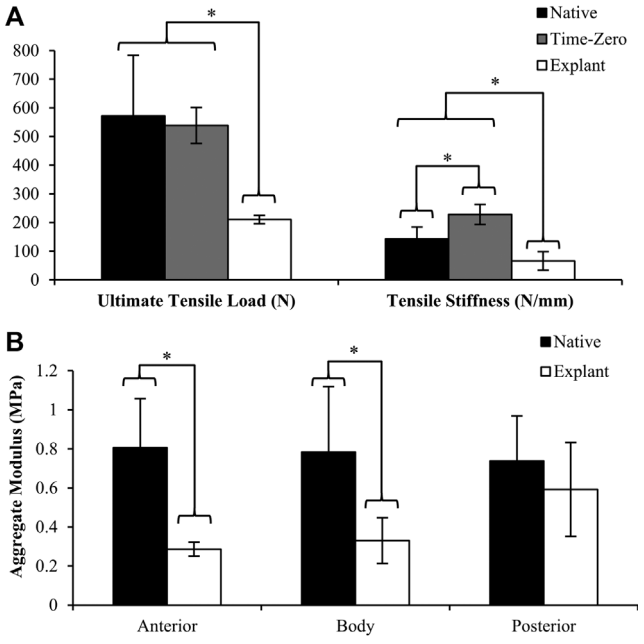

Figure 4. (A) Ultimate tensile load and tensile stiffness of 52-week explants (n = 3) compared with native ovine menisci and time-zero scaffolds (n = 4 each). (B) Aggregate modulus of 52-week explants (n = 3 anterior/posterior, n = 4 body) compared with native ovine menisci (n = 4 per region). Mean ± SD. *Statistically significant difference.

to be evenly dispersed through the interior of the cross section. The surfaces of the explants were composed of new tissue that did not contain fibers.

Significant cellular infiltration was seen throughout the explants, with no noticeable differences in concentration between the inner and outer margins. Cells near polymer fibers tended to display an elongated shape, while cells along the inner margin experienced more circular fibrochondrocytic shapes. There were areas of dense ECM deposition and organization in the posterior region of all 4 explants, and the body region contained moderately less organization. The anterior region contained little noticeable ECM organization as a large portion of the area was still occupied by fibers. The explant ECM was not as organized as that of the native meniscus, but the body and posterior regions did have areas of aligned collagen fibers similar to native tissue (Figure 5). Blood vessels were observed in all 3 regions and in both the inner and outer meniscus (see Figure 5, body, 200×). There was a slight presence of inflammatory cells, mainly monocytes and neutrophils. These cells were found primarily surrounding the pDTDDD fibers, with the anterior region having the greatest inflammatory response.

Immunohistochemical staining showed that COL-1 was found primarily in the outer two-thirds of all 3 explant regions and was more present and organized in the body and posterior regions than in the anterior region. In all regions, COL-1 was frequently observed surrounding any remaining polymer fiber. The organized regions of COL-1

Downloaded from ajs.sagepub.com at RUTGERS UNIV on April 5, 2016

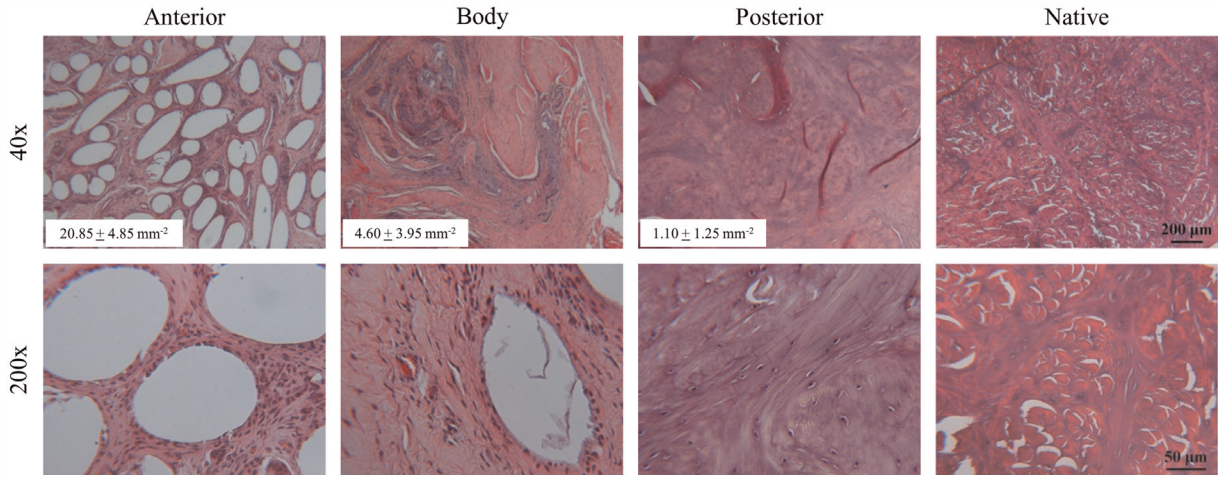

Figure 5. Hematoxylin and eosin–stained slices from the anterior, body, and posterior regions of 52-week explants, compared with native meniscus at low and high magnification. Fiber densities (fibers/mm^2; mean ± SD) are shown in the bottom left corner of 3 explant images.

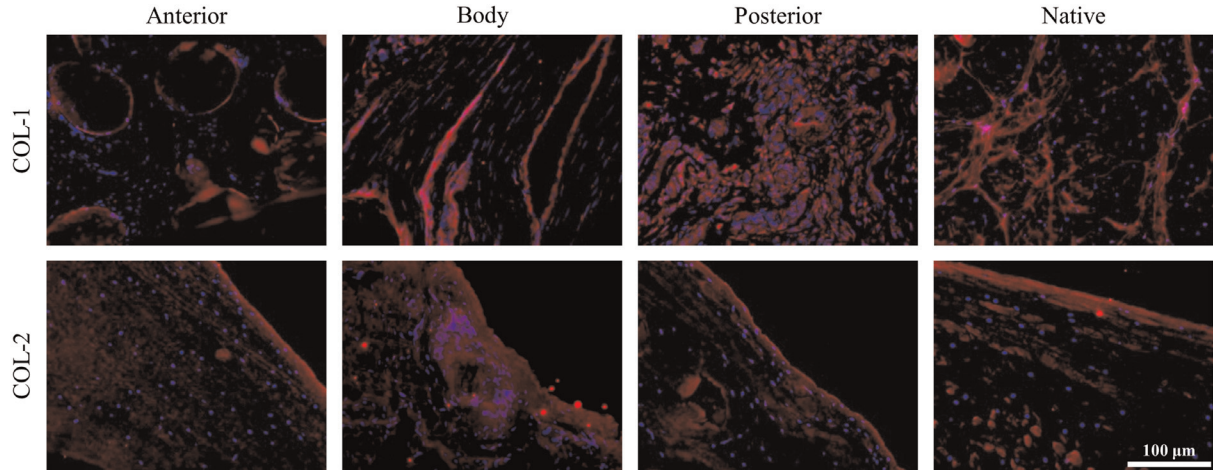

Figure 6. Collagen type 1 (COL-1; outer two-thirds) and COL-2 (inner third) immunohistochemical staining. Collagen (red) with cell nuclei (blue) for native and explant tissue.

in the ECM were almost always paired with elongated nuclei (Figure 6). COL-2 was primarily found near the inner margin of explants, with a higher concentration at the tissue surface. No considerable differences were observed in COL-2 content between the anterior, body, and posterior regions of the explants. The inner margin of explants contained rounder cell nuclei than the outer two-thirds. COL-1 images from the outer two-thirds and COL-2 images from the inner margin are shown in Figure 6 for native and explant tissue.

Biochemical Content

After digestion with papain, several implant samples had small strands remaining, indicating the presence of polymer fibers. Collagen and S-GAG percentage per dry weight are shown in Figure 7. No statistical differences existed between explant and native tissue within each region for both biochemical tests. However, the average collagen content of all explant plugs was 64.8% that of native tissue, a significant difference ($P < .001$). Collagen and S-GAG content did not vary significantly by region, but the posterior region (1.14% ± 0.26%) had a higher percentage of S-GAG than did the anterior (0.76% ± 0.17%) and body (1.01% ± 0.30%) regions.

Articular Cartilage Evaluation

Macroscopic observations showed all 7 experimental sheep exhibited only superficial abrasions to both the femoral condyle and tibial plateau. These were centralized to the Central-Central region, as described by the ICRS, or on both surfaces at the point of contact in standing position.

Downloaded from ajs.sagepub.com at RUTGERS UNIV on April 5, 2016

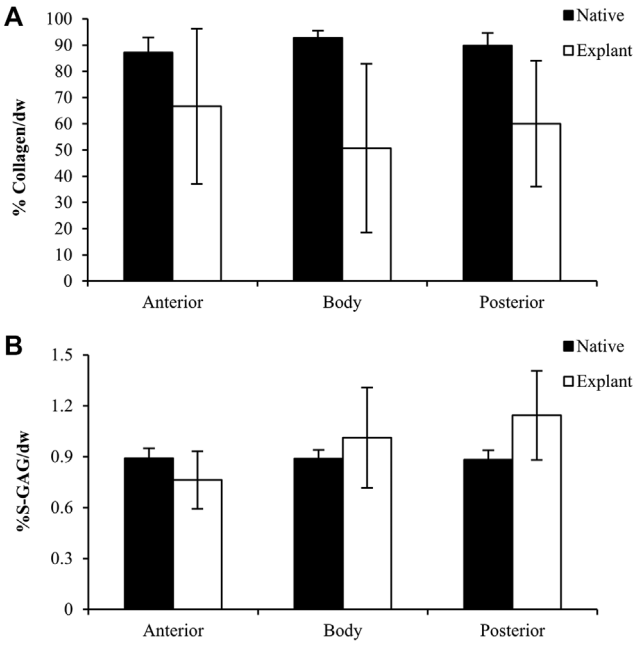

Figure 7. Collagen and sulfated-glycosaminoglycan (S-GAG) content as a percentage of dry weight (dw) tissue in the anterior, body, and posterior regions of native and explant tissue. Mean ± SD.

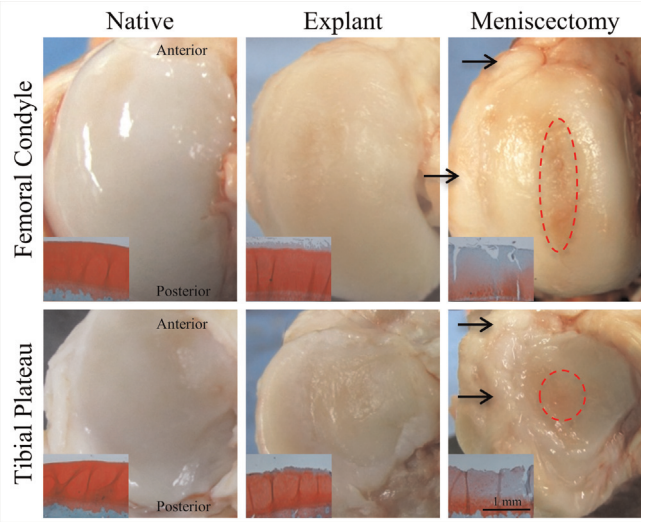

Figure 8. Articular surfaces of native joint, 52-week explant joint, and 52-week meniscectomy joint. Severe damage is highlighted by red dotted ellipses, and osteophytes are highlighted by black arrows. Insets: Representative histological images of cartilage used to determine Mankin scores.

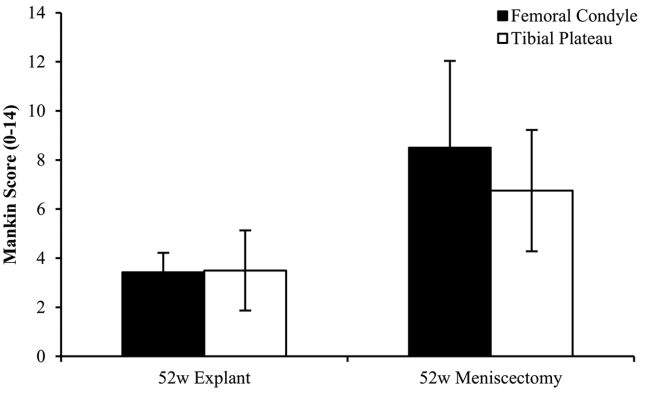

Figure 9. Femoral condyle and tibial plateau Mankin scores (out of 14) for explant and meniscectomy groups at 52 weeks. Mean ± SD.

The tibial plateau directly under the meniscus explants remained pristine. Both meniscectomy sheep exhibited visibly deeper lesions, with 1 sheep experiencing damage down to the bone. Superficial abrasions were also seen on a greater area of meniscectomy surfaces than on experimental surfaces. In addition, slight osteophytic growth was noted on both meniscectomy surfaces, even underneath the weak scar tissue that grew into the empty space. Sample articular surfaces of the experimental and meniscectomy groups are compared with a native joint in Figure 8.

Histological assessment (Figure 8, insets) showed that the experimental group experienced only superficial cartilage damage to the femoral condyles and tibial plateaus, never deeper than 20% of the cartilage thickness. The meniscectomy group experienced damage to the bone in 1 animal and damage to the radial zone of the cartilage in the other. Slight hypocellularity was seen at the surface of experimental groups, as well as a slight reduction in the proteoglycan stain. These changes were more severe in the meniscectomy group. All tidemarks were intact, except for 1 of the 2 meniscectomy femoral condyles. Mankin scores were lower for both the femoral condyles and the tibial plateaus in the experimental group than for those in the meniscectomy group (Figure 9).

DISCUSSION

The purpose of this study was to assess the functionality of a novel pDTDDD fiber-reinforced collagen-hyaluronan sponge for total meniscus replacement in a 52-week animal model with regard to mechanics, histology, ECM composition, and cartilage protection. To our knowledge, this study is the first to test all of these criteria with a tissue-engineered total meniscus substitute for at least 52 weeks.

While several constructs have shown short-term success in animal models,[7] studies longer than 24 weeks have typically resulted in implant ruptures or joint deterioration.[16,24,25] One of the most common reasons for these failures is inadequate tensile strength in these implants. Based on the tensile stiffness of the native ovine meniscus from this study, an average cross-sectional area of ~25 mm^2,[6] and a strain of 8% at maximum compressive load,[36] the maximum circumferential load that an ovine meniscus would encounter would be ~120 N. Although the ultimate tensile loads of all three 52-week

Downloaded from ajs.sagepub.com at RUTGERS UNIV on April 5, 2016

explants were less than half of their time-zero value, they were well above this 120-N functional tensile load. This explains the ability for all 7 explants to remain intact. It is important to note that these tensile properties are not indicative of the entire meniscus, only the body region. Because of the narrowing of the explant body regions in this study, the anterior and posterior regions would be expected to have significantly higher ultimate tensile loads and tensile stiffnesses.

With tensile stiffness values that were approximately half that of native tissue, the 52-week explants displaced more than native menisci under loading conditions, likely causing permanent narrowing in the body region. To date, no other study has analyzed the tensile properties at or past 52 weeks, but other studies have experienced similar narrowing or extrusion.[18,25] The addition of polymer fibers to the implant in this study was intended to help prevent narrowing; however, even though these changes made the scaffold stronger, it also made the scaffold thicker, with geometry less like the native meniscus. Compression of the femoral condyle onto the thicker implant may have caused the inner margin of the scaffold to be pushed out, causing narrowing in the body region. Therefore, our future studies with this scaffold will give greater care to the geometry of the final product.

While more narrowing occurred in the 52-week study than at earlier time points (2/8 at 16 weeks, 3/8 at 32 weeks),[31] tensile properties remained fairly consistent from 16 weeks onward. The ultimate tensile load and tensile stiffness in this study (210.4 ± 14.0 N; 66.1 ± 32.5 N/mm) were only 11.1% and 10.4% lower than that at 32 weeks (236.7 ± 39.3 N; 73.8 ± 18.4 N/mm). Because the fibers have degraded significantly by 16 weeks,[42] they are contributing less to the mechanics of the scaffold, and the regenerated tissue is assuming a larger portion of the circumferential stresses. Therefore, past 52 weeks, the tensile mechanics of this tissue are not expected to decrease.

The evidence of ECM deposition was also suggested by the confined compressive creep data. The average aggregate modulus at 52 weeks (0.40 ± 0.19 MPa) was about half that of native tissue, but this value was more than double that of time-zero scaffolds from our previous study (~0.15 MPa[31]). The increase in mechanics can be attributed to tissue deposition and organization. This theory is further supported by a slight increase compared with explants from earlier time points (16 weeks: 0.33 ± 0.07 MPa; 32 weeks: 0.33 ± 0.09 MPa).[31] Most of the previous in vivo meniscus studies did not report compressive values,[23,25] especially in confined creep. With regard to a compressive equilibrium modulus, Gruchenberg et al[15] showed increases from time-zero silk fibroin scaffolds (~45 kPa) to 6-month explants (76 kPa) toward native meniscus values (95 kPa), albeit for a partial meniscus replacement. Tienen et al[41] also reported significant increases in compressive moduli of 6-month explants from time-zero porous polymer scaffolds but was able to achieve modulus values that were approximately only 38% of native tissue. To our knowledge, no meniscus study has been able to obtain compressive moduli greater than native tissue, but increasing the initial compressive stiffness of the scaffolds could be a potential avenue for doing so.

The collagen sponge used in the study allows for rapid cell infiltration and attachment, followed by a more gradual remodeling process. In addition, the degradation of the pDTDDD fiber allows for additional cell infiltration and ECM deposition. This degradation was verified by the reduction in fibers from 32-week explants to 52-week explants. In the 52-week explants, the anterior region contained ~21 fibers per mm^2, estimated to be 64% of the time-zero density, whereas the fiber densities of the body and posterior regions were only 14% and 3%, respectively. Since the junction of the body and posterior regions typically experiences the greatest circumferential strain,[10] the fibers in these 2 regions most likely degraded more rapidly because of loading. The difference in fiber density can most likely be attributed to the least amount of strain being placed on the anterior region.

The strain profile may also explain the region-dependent ECM organization of the explants. The anterior region of the explants was the least organized and contained the least COL-1, perhaps because of the least total strain in this region. In contrast, since the posterior region of the meniscus experiences the highest combination of strains,[10] a greater degree of tissue deposition and organization occurred in this region. Many of the COL-1 fiber bundles and tie fibers seen in the explants resembled those found in native tissue. While other studies have not emphasized differences in ECM properties by region, several have also been able to induce a similar microarchitecture to the native meniscus.[26,35] Specifically, in this study, we observed COL-1 in the outer two-thirds and COL-2 in the inner third in orientations and quantities similar to native tissue. In addition, the presence of aligned collagen fiber bundles was more apparent in 52-week explants when compared with earlier time points,[31] suggesting that the scaffold continues to be remodeled.

While biochemical data were not available from the earlier time points, collagen content approached native tissue values and was vastly increased from the time-zero scaffold, which consisted of ~14% collagen based on scaffold and fiber weights. S-GAG content slightly above native tissue was also observed (~10% greater), with the posterior region showing the highest content. The presence of S-GAGs at native levels in our explants may also indicate similar levels of the proteoglycan aggrecan. A larger proteoglycan content will improve osmotic properties, correlating with the improved compressive moduli. The elevated amount of stress on the posterior region may have caused the cells in this region to synthesize more proteoglycans and the associated S-GAGs for compressive resistance. On the other hand, the lower stress on the anterior region most likely resulted in it having the least S-GAG. Regardless, all regions were comparable with native tissue. This development of the ECM is contingent upon the location and phenotype of the cells.

The qualitative cellular observations suggest the presence of fibrochondrocytes. The elongated shape of cells in proximity to fibers suggests that these cells have experienced tension, making them fibroblastic. Elongated nuclei were shown in the immunohistochemistry, especially near aligned fiber bundles in the outer two-thirds, indicative of

Downloaded from ajs.sagepub.com at RUTGERS UNIV on April 5, 2016

COL-1 expression by fibroblasts. The rounded shape of cells throughout the rest of the scaffold, especially on the inner margin, implies a response to compression. COL-2 was expressed by many of these cells, indicating a cartilage-like tissue. Other studies have obtained very similar cellular phenotypes, either through cell seeding or growth factor addition.[21,23] For example, Lee et al[26] induced fibrochondrocytic differentiation of mesenchymal stem cells and collagen expression with growth factors, and Kon et al[25] showed increased cartilage metaplasia by seeding autologous chondrocytes onto their scaffold. To our knowledge, the ability of our scaffold to display these properties without any cellular or growth factor addition is unique. The minimal inflammatory response implies that the by-products of the polymer degradation were nontoxic and nonacidic, consistent with previous reports on degradation of polyarylates.[20]

Perhaps the most important requirement of meniscus replacement is protecting the articular surfaces. While scar tissue ingrowth with the approximate shape of the meniscus was observed in the meniscectomy group of this study, this group experienced significant joint deterioration, including damage deep into at least the radial zone and the presence of osteophytes. It is apparent that this weak scar tissue was not able to distribute loads, allowing for significant cartilage damage to occur. In contrast, the explant group displayed markedly less cartilage damage. While joint preservation was observed in many short-term studies,[24,26] this is one of the only studies of at least 52 weeks to show improvement over meniscectomy.[16,24,25] Even with a partial meniscus replacement, Maher et al[27] showed no significant differences in cartilage protection between implantation with Actifit and partial meniscectomy in sheep in a 12-month study. Furthermore, our scaffold was able to avoid progressive cartilage damage between time points that is frequently found in the both partial and total meniscus replacements.[16,24,45] For example, Hannink et al[16] showed only moderate cartilage damage at 6 months, but by 24 months, Mankin scores were higher than those of meniscectomy controls. Their 6-month femoral condyle and tibial plateau Mankin scores were 6 and 6.5, respectively, which were almost double the values found in this 52-week study. Moreover, femoral condyle Mankin scores at 52 weeks (3.43 $\pm$ 0.79) were comparable with those at 16 weeks (3.71 $\pm$ 2.50) and 32 weeks (3.14 $\pm$ 2.28), showing that cartilage damage was not progressing. Therefore, the reduction in cartilage damage for the implant group versus meniscectomy and the maintenance of the articular surfaces with time make the results of this study distinctive.

There were a few limitations in this study. In an effort to reduce the number of animals used, 8 experimental but only 2 untreated meniscectomy sheep were used, as we had previously established the deleterious effects of that procedure on sheep articular cartilage at 16 and 32 weeks.[31] Because of the exclusion of 1 sheep and the existence of 2 explant analysis groups, only 3 implants were included in some of the analyses. Ultimate tensile testing was performed only on the body region because of gripping constraints. In addition, because of the constraints of the explant groups (Figure 2), body plugs were taken from different animals than the anterior and posterior plugs, adding a potential element of variability. Last, the sheep used in this study returned to a standing position hours after surgery, which is not representative of the restrictions on movement and activity after procedures in humans. A nonweightbearing recovery period might allow for matrix remodeling to initiate without loading that could cause rupture, extrusion, thinning, or narrowing.

Our quasi-woven meniscus implant was able to remain intact, maintain functional tensile properties, exhibit fibrochondrocytic cells, continue ECM deposition and organization, and protect the articular surfaces. To our knowledge, this is the first study to successfully show these properties in a total meniscus replacement for at least 1 year in a large animal model. Future work will test a modified implant for longer than 52 weeks to determine if tissue organization and mechanics that are more comparable with the native meniscus are achieved. Furthermore, an implant with the corresponding size and shape of the human meniscus will be developed and evaluated.

ACKNOWLEDGMENT

The authors thank the Orthopaedic Research Laboratory, the vivarium staff, and especially Barbara Perry for their assistance with the surgeries and postoperative care. They also thank Rita Hahn and Marion Gordon, from the Earnest Mario School of Pharmacy Rutgers–Robert Wood Johnson Medical School, for their support and assistance with immunohistochemistry.

REFERENCES

1. Allen PR, Denham RA, Swan AV. Late degenerative changes after meniscectomy: factors affecting the knee after operation. *J Bone Joint Surg Br*. 1984;66(5):666-671.
2. Arnoczky SP, Warren RF. Microvasculature of the human meniscus. *Am J Sports Med*. 1982;10(2):90-95.
3. Baek J, Jin S, Sovani S, Chen X, D'Lima DD, Grogan SP. Meniscal tissue engineering: cell encapsulation of electrospun collagen. Paper presented at: Orthopaedic Research Society Annual Meeting, 2014; New Orleans, LA. http://www.ors.org/Transactions/60/0225.pdf.
4. Balint E, Gatt CJ Jr, Dunn MG. Design and mechanical evaluation of a novel fiber-reinforced scaffold for meniscus replacement. *J Biomed Mater Res A*. 2012;100(1):195-202.
5. Bourke SL, Kohn J. Polymers derived from the amino acid L-tyrosine: polycarbonates, polyarylates and copolymers with poly(ethylene glycol). *Adv Drug Deliv Rev*. 2003;55(4):447-466.
6. Chevrier A, Nelea M, Hurtig MB, Hoemann CD, Buschmann MD. Meniscus structure in human, sheep, and rabbit for animal models of meniscus repair. *J Orthop Res*. 2009;27(9):1197-1203.
7. Chiari C, Koller U, Dorotka R, et al. A tissue engineering approach to meniscus regeneration in a sheep model. *Osteoarthritis Cartilage*. 2006;14(10):1056-1065.
8. de Groot JH, de Vrijer R, Pennings AJ, Klompmaker J, Veth RP, Jansen HW. Use of porous polyurethanes for meniscal reconstruction and meniscal prostheses. *Biomaterials*. 1996;17(2):163-173.
9. Efe T, Getgood A, Schofer MD, et al. The safety and short-term efficacy of a novel polyurethane meniscal scaffold for the treatment of segmental medial meniscus deficiency. *Knee Surg Sports Traumatol Arthrosc*. 2012;20(9):1822-1830.

Downloaded from ajs.sagepub.com at RUTGERS UNIV on April 5, 2016

10. Freutel M, Seitz AM, Galbusera F, et al. Medial meniscal displacement and strain in three dimensions under compressive loads: MR assessment. *J Magn Reson Imaging*. 2014;40(5):1181-1188.
11. Freymann U, Endres M, Neumann K, Scholman HJ, Morawietz L, Kaps C. Expanded human meniscus-derived cells in 3-D polymer-hyaluronan scaffolds for meniscus repair. *Acta Biomater*. 2012;8(2):677-685.
12. Garrett WE Jr, Swiontkowski MF, Weinstein JN, et al. American Board of Orthopaedic Surgery Practice of the Orthopaedic Surgeon: Part-II, certification examination case mix. *J Bone Joint Surg Am*. 2006;88(3):660-667.
13. Gatt CJ, Balint EA, Dunn MG, inventors; Rutgers, The State University of New Jersey, assignee. Bioresorbable tissue engineered fibrocartilage replacement with three-dimensional matrix of fibers. US patent 8,623,085. January 7, 2014.
14. Grogan SP, Chung PH, Soman P, et al. Digital micromirror device projection printing system for meniscus tissue engineering. *Acta Biomater*. 2013;9(7):7218-7226.
15. Gruchenberg K, Ignatius A, Friemert B, et al. In vivo performance of a novel silk fibroin scaffold for partial meniscal replacement in a sheep model. *Knee Surg Sports Traumatol Arthrosc*. 2015;23(8):2218-2229
16. Hannink G, van Tienen TG, Schouten AJ, Buma P. Changes in articular cartilage after meniscectomy and meniscus replacement using a biodegradable porous polymer implant. *Knee Surg Sports Traumatol Arthrosc*. 2011;19(3):441-451.
17. Hede A, Larsen E, Sandberg H. The long term outcome of open total and partial meniscectomy related to the quantity and site of the meniscus removed. *Int Orthop*. 1992;16(2):122-125.
18. Holloway JL. *Development and Characterization of UHMWPE Fiber-Reinforced Hydrogels For Meniscal Replacement* [PhD thesis]. Philadelphia, PA: Drexel University; 2012.
19. Holloway JL, Lowman AM, VanLandingham MR, Palmese GR. Interfacial optimization of fiber-reinforced hydrogel composites for soft fibrous tissue applications. *Acta Biomater*. 2014;10(8):3581-3589.
20. Hooper KA, Macon ND, Kohn J. Comparative histological evaluation of new tyrosine-derived polymers and poly (L-lactic acid) as a function of polymer degradation. *J Biomed Mater Res*. 1998;41(3):443-454.
21. Ionescu LC, Lee GC, Huang KL, Mauck RL. Growth factor supplementation improves native and engineered meniscus repair in vitro. *Acta Biomater*. 2012;8(10):3687-3694.
22. Ionescu LC, Mauck RL. Porosity and cell preseeding influence electrospun scaffold maturation and meniscus integration in vitro. *Tissue Eng Part A*. 2013;19(3-4):538-547.
23. Kang SW, Son SM, Lee JS, et al. Regeneration of whole meniscus using meniscal cells and polymer scaffolds in a rabbit total meniscectomy model. *J Biomed Mater Res A*. 2006;78(3):659-671.
24. Kelly BT, Robertson W, Potter HG, et al. Hydrogel meniscal replacement in the sheep knee: preliminary evaluation of chondroprotective effects. *Am J Sports Med*. 2007;35(1):43-52.
25. Kon E, Filardo G, Tschon M, et al. Tissue engineering for total meniscal substitution: animal study in sheep model—results at 12 months. *Tissue Eng Part A*. 2012;18(15-16):1573-1582.
26. Lee CH, Rodeo SA, Fortier LA, Lu C, Erisken C, Mao JJ. Protein-releasing polymeric scaffolds induce fibrochondrocytic differentiation of endogenous cells for knee meniscus regeneration in sheep. *Sci Transl Med*. 2014;6(266):266ra171.
27. Maher SA, Rodeo SA, Doty SB, et al. Evaluation of a porous polyurethane scaffold in a partial meniscal defect ovine model. *Arthroscopy*. 2010;26(11):1510-1519.
28. Makris EA, Hadidi P, Athanasiou KA. The knee meniscus: structure-function, pathophysiology, current repair techniques, and prospects for regeneration. *Biomaterials*. 2011;32(30):7411-7431.
29. Mandal BB, Park SH, Gil ES, Kaplan DL. Multilayered silk scaffolds for meniscus tissue engineering. *Biomaterials*. 2011;32(2):639-651.
30. Mankin HJ, Dorfman H, Lippiello L, Zarins A. Biochemical and metabolic abnormalities in articular cartilage from osteo-arthritic human hips. II. Correlation of morphology with biochemical and metabolic data. *J Bone Joint Surg Am*. 1971;53(3):523-537.
31. Merriam AR, Patel JM, Culp BM, Gatt CJ, Dunn MG. Successful total meniscus reconstruction using a novel fiber-reinforced scaffold: a 16- and 32-week study in an ovine model. *Am J Sports Med*. 2015;43(10):2528-2537.
32. Mow V, Ratcliffe A. Structure and function relationships of the menisci of the knee. In: Mow V, Arnoczky S, Jackson D, eds. *Knee Meniscus: Basic and Clinical Foundations*. New York, NY: Raven Press; 1992:37-57.
33. Mow VC, Kuei SC, Lai WM, Armstrong CG. Biphasic creep and stress relaxation of articular cartilage in compression? Theory and experiments. *J Biomech Eng*. 1980;102(1):73-84.
34. Neuman RE, Logan MA. The determination of hydroxyproline. *J Biol Chem*. 1950;184(1):299-306.
35. Puetzer JL, Ballyns JJ, Bonassar LJ. The effect of the duration of mechanical stimulation and post-stimulation culture on the structure and properties of dynamically compressed tissue-engineered menisci. *Tissue Eng Part A*. 2012;18(13-14):1365-1375.
36. Richards CJ, Gatt CJ Jr, Langrana N, Calderon R. Quantitative measurement of human meniscal strain. Paper presented at: Orthopaedic Research Society Annual Meeting; February 2003; New Orleans, LA. http://www.ors.org/Transactions/49/0649.pdf.
37. Rodeo SA. Meniscal allografts: where do we stand? *Am J Sports Med*. 2001;29(2):246-261.
38. Steadman JR, Rodkey WG. Tissue-engineered collagen meniscus implants: 5- to 6-year feasibility study results. *Arthroscopy*. 2005;21(5):515-525.
39. Stone KR, Steadman JR, Rodkey WG, Li ST. Regeneration of meniscal cartilage with use of a collagen scaffold: analysis of preliminary data. *J Bone Joint Surg Am*. 1997;79(12):1770-1777.
40. Sweigart MA, Athanasiou KA. Toward tissue engineering of the knee meniscus. *Tissue Eng*. 2001;7(2):111-129.
41. Tienen TG, Heijkants RG, de Groot JH, et al. Replacement of the knee meniscus by a porous polymer implant: a study in dogs. *Am J Sports Med*. 2006;34(1):64-71.
42. Tovar N, Bourke S, Jaffe M, et al. A comparison of degradable synthetic polymer fibers for anterior cruciate ligament reconstruction. *J Biomed Mater Res A*. 2010;93(2):738-747.
43. van Tienen TG, Heijkants RG, Buma P, de Groot JH, Pennings AJ, Veth RP. Tissue ingrowth and degradation of two biodegradable porous polymers with different porosities and pore sizes. *Biomaterials*. 2002;23(8):1731-1738.
44. Welsing RT, van Tienen TG, Ramrattan N, et al. Effect on tissue differentiation and articular cartilage degradation of a polymer meniscus implant: a 2-year follow-up study in dogs. *Am J Sports Med*. 2008;36(10):1978-1989.
45. Zur G, Linder-Ganz E, Elsner JJ, et al. Chondroprotective effects of a polycarbonate-urethane meniscal implant: histopathological results in a sheep model. *Knee Surg Sports Traumatol Arthrosc*. 2011;19(2):255-263.

For reprints and permission queries, please visit SAGE's Web site at http://www.sagepub.com/journalsPermissions.nav.

Downloaded from ajs.sagepub.com at RUTGERS UNIV on April 5, 2016